# Investigation of pressing process for large and thick blades of Francis turbines

**Zhengkun Feng[a], Henri Champliaud[a], Louis Mathieu[b], Michel Sabourin[b], Van Ngan Lê[a]**

*a. Department of Mechanical Engineering, Ecole de technologie superieure, 1100 Notre-Dame Street West, Montreal, Quebec, H3C 1K3, Canada*
*b. Alstom Renewable Power, Hydro, Global Technology Centre, Alstom Hydro Canada Inc., 1350 St-Roch Road, Sorel-Tracy, Quebec, J3P 5P9, Canada*

## Résumé :

*Le procédé de pressage est très reconnu pour déformer des tôles minces. Cependant, le mécanisme de ce procédé pour les plaques épaisses en acier à haute résistance et à haute température mérite plus d'attention. Le procédé est caractérisé par des comportements thermomécaniques, de fortes non-linéarités, des déformations tridimensionnelles et instables. Dans cet article, un modèle du procédé de fabrication des aubes larges et épaisses pour des turbines Francis est proposé. L'analyse du procédé est basée sur la méthode des éléments finis sous ANSYS et LS-DYNA. L'ensemble du procédé de fabrication se compose du pressage de l'aube à partir d'une plaque plane, du retour élastique après formage et du refroidissement de l'aube pressée à une température de 800 °C jusqu'à la température ambiante. Finalement, l'évolution de la distribution des contraintes est aussi analysée.*

## Abstract :

*Hot pressing process is very popular for thin plates in metal forming. However, the process mechanism for thick plates of high strength steel at high temperature deserves more investigations. The process is characterized by thermo-mechanical behaviors, three-dimensional unsteady deformations and high nonlinearity. In this paper, the model of the process for manufacturing large and thick blades of Francis turbines is proposed. The process analysis is based on finite element method under ANSYS and LS-DYNA platforms to get better understanding of the process. The whole process consists of the pressing forming of a blade from a flat blank, the springback after the forming and the cooling of the pressed blade from high temperature to room temperature. Investigation of the stress evolution is also performed.*

**Keywords: Hot pressing, Finite element analysis, Thick and curved plate forming, Initial residual stress, Springback, Cooling**

## 1 Introduction

Pressing process has many advantages over conventional casting process [1, 2]. Casting defects may happen due to metal contraction and trapped gas during cooling and solidification [3, 4]. Consequently, the pressing process is widely applied in manufacture, such as automotive, shipbuilding and civil engineering [5-7]. Francis turbine blades of hydropower plants can be produced from thick plates by pressing process. The process to produce a blade from a flat plate consists of optimal blank design and the following sub-processes. After obtaining the geometrical data of the flat blank by optimal blank design [8], the blank passes successively through plate pressing [9], the springback of the pressed shape, the cooling of the pressed blade to room temperature, and finally the blade machining by a 5-axis CNC milling machine to obtain the desired hydraulic profile and thickness at each location [10]. The workpiece has residual stress at the end of each subprocess which is the initial stress of the next subprocess. The history of stress distribution through all the process may affect the residual stress of the workpiece. Recently, Deng and Kiyoshima have investigated the influence of initial residual stress induced by heat treatment on the final residual stress of laser welding [11]. The effect of initial residual stresses on thermal strain evolution in tube during welding has been investigated by De Strycker et al. [12]. Park and Lee have investigated the effects of initial stress due to plate forming on the residual stress of welding process [13]. Huang and Lu have analysed the influence of initial axial residual stress on the stress and strain of a product assembled by welding a cylinder and a semi-sphere [14]. The effects of initial stress on crack driving force of girth welded pipe with internal circumferential cracks have been investigated by Sisan and Motarjemi [15]. However, the initial stress is often neglected in the developed numerical models [11]. This study presents process modelling and simulations of three sub-processes: the plate pressing, the springback of pressed shape and the cooling of the pressed blade to room temperature.

# 2 Process modeling and simulations

The process modelling was based on the finite element method under ANSYS and ANSYS/LS-DYNA platforms. The model for hot pressing process was built under ANSYS/LS-DYNA platform using explicit time integration scheme. Both models for springback and blade cooling were built under ANSYS platform using implicit time integration scheme.

## 2.1 Pressing process

The numerical model for simulating pressing process for thick plates is shown in Fig. 1. The model consisted of the optimal flat blank, a punch and a die which were meshed with four-node shell elements with five integration points through thickness. A uniform of temperature of 800 $^{o}$C of the blank was assumed during the pressing. The elastic perfectly plastic material as given in Fig. 2 and Table 1 at temperature of 800 $^{o}$C was used in the material model of the flat blank. The blank had a middle surface with an area of 4.09 m$^2$. The mesh of the blank had 3444 elements and 3569 nodes. The punch and the die were assumed as rigid bodies. The contact type on the contact surfaces between the punch, the die and the blank was automatic node-to-surface contact. The static and dynamic friction coefficients between the blank and the punch and between the blank and the die were 0.2, respectively. For the sake of CPU time, the simulation time was selected as 1 second. The model had the capacity to form flat blanks with maximal thickness of 80 mm to the designed blades. Figure 3 shows the shape of a blade achieved from a blank thickness of 80 mm with the FE model. Figure 4 shows the von Mises stress distribution on the formed blade obtained from an optimal flat blank. The zone of high curvature had the maximal stress of 134 MPa which was the yield stress.

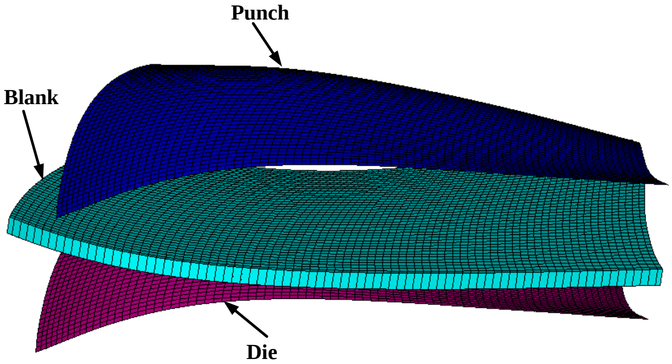


FIG. 1 – Pressing process model based on finite element method.

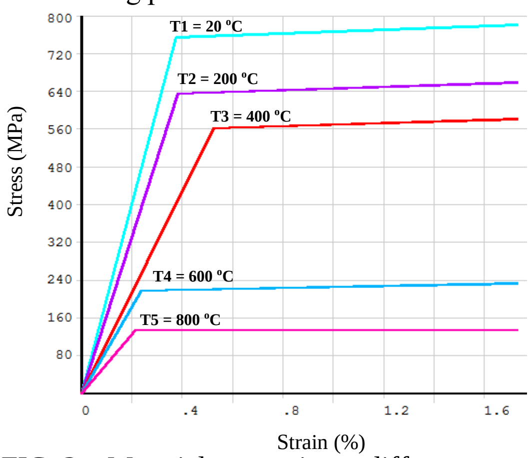


FIG. 2 – Material properties at different temperatures.

Table 1 –Mechanical properties of blades

| | Temperature (°C) | | | | |
|---|---|---|---|---|---|
| | 20 | 200 | 400 | 600 | 800 |
| Elastic modulus (GPa) | 200 | 180 | 166 | 107 | 92 |
| Yield stress (MPa) | 754 | 635 | 562 | 218 | 134 |
| Poisson's ratio | 0.3 | 0.3 | 0.3 | 0.3 | 0.3 |
| Density ($Kg/m^3$) | 7850 | 7850 | 7850 | 7850 | 7850 |

Table 2 –Thermal properties of blades

| | Temperature (°C) | | | | |
|---|---|---|---|---|---|
| | 20 | 200 | 400 | 600 | 800 |
| Thermal conductivity (W/m °C) | 51 | 49.5 | 48 | 42 | 37 |
| Specific heat (J/kg °C) | 480 | 500 | 510 | 580 | 700 |
| Convection coefficient ($W/m^2$ °C) | 9.5 | 11.8 | 16.3 | 30.8 | 54.8 |
| Thermal expansion coefficient ($x10^{-6}$ $°C^{-1}$ ) | 12.18 | 12.18 | 12.66 | 13.47 | 14.41 |

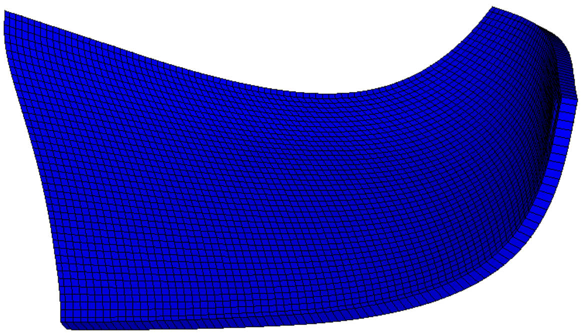

FIG. 3 –Shape of the blade obtained with FE model prior to springback.

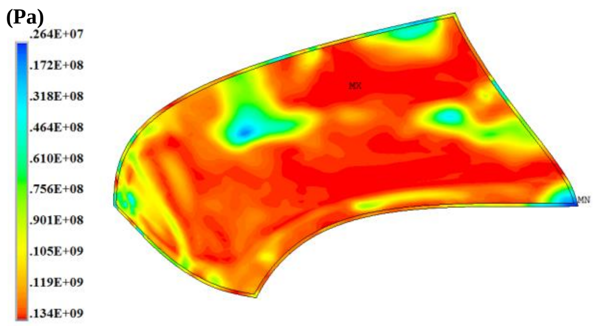


FIG. 4 – Residual von Mises stress distribution prior to springback.

## 2.2 Springback after pressing process

The final shape and the residual stress of the workpiece obtained by the pressing model under ANSYS/LS-DYDA platform in section 2.1 were brought to ANSYS to perform springback. The model kept only the mesh of the workpiece with the same connectivity, but with the coordinates of the nodes updated by the final shape of the workpiece in section 2.1. The punch and die were no longer considered at this stage. The residual stress obtained in section 2.1 was used as initial stress in this section. The new boundary conditions were defined by three corner points which defined the coordinate system as follows: the translation degrees of freedom in X, Y and Z directions for one point were imposed to zero; the translation degrees of freedom in Y and Z directions for the second point were imposed to zero, the translation degree of freedom in Z direction for the third point was imposed to zero. Figure 5 shows the von Mises stress distribution over the workpiece after springback. In comparison with the distribution shown in Fig. 4, the area size with the maximal von Mises stress had significantly decreased.

## 2.3 Cooling process from 800 °C to room temperature

As in section 2.2, the final shape and the residual stress of the workpiece obtained after springback was used as the geometry for the model. The material properties at different temperatures from 20 °C to 800 °C are shown in Fig. 2, Table 1 and Table 2. The material was assumed as elastic perfectly plastic at 800 °C and elasto-plastic at the other temperatures. The model kept also the mesh of the workpiece with the same connectivity, but with the coordinates of the nodes updated by the final shape after springback. Similarly, the residual stress obtained in section 2.2 was used as initial stress in this section. The boundary conditions for the structural model were not changed. The computational steps were uncoupled, meaning that the thermal solution was performed and that the temperature distribution was used as boundary loads for the structural solution. Natural convection boundary conditions for the thermal model were imposed on the six surfaces (the four edges, intrados and extrados) with ambient fluid temperature of 20 °C. It was assumed that the initial temperature was uniform with a value of 800 °C. Firstly, simulation with the thermal model for cooling was performed to obtained temperature distribution at each time step. Figure 6 shows the temperature distributions 372 seconds and 3.2 hours after cooling started. Then, the structural solution was performed with the temperature loads at each step obtained from the thermal model. The boundary conditions for the structural model were the same as in section 2.2. Figure 7 shows the von Mises stress distribution 372 seconds after cooling started which corresponded to the temperature distribution in Fig. 6a. Figure 8 shows the von Mises stress distribution over the workpiece after cooling ends. Figure 8a shows the redistribution of von Mises stress in comparison with the distribution in Fig. 5. The von Mises stress in zone A, was more than 134 Mpa. Although the maximal von Mises stress had increased due to the increasing of material yield stresses when the temperature decreased (Fig. 8b). However, the maximal value was far below the room temperature yield stress of 754 Mpa.

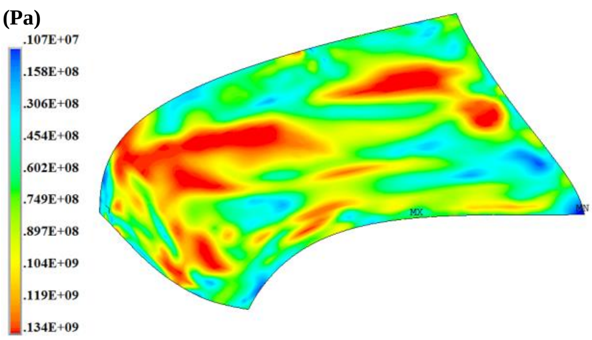


FIG. 5 – Residual stress distribution after spring back.

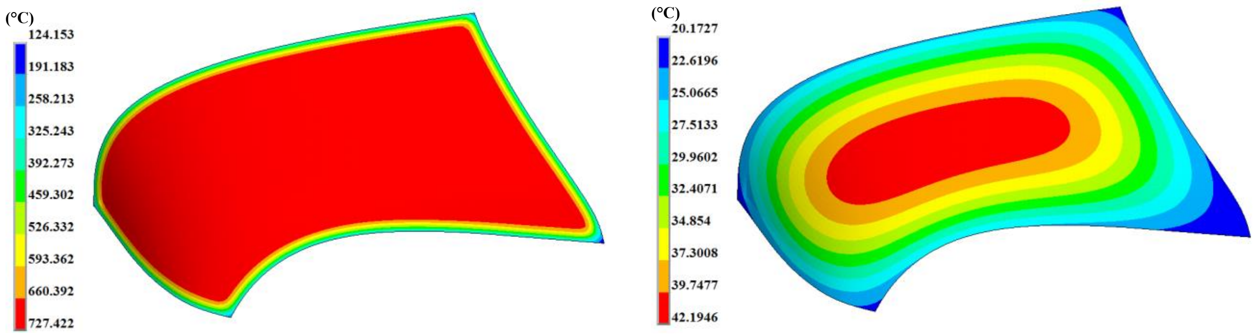


(a) 372 seconds after cooling started. (b) 3.2 hours after cooling started

FIG. 6 –Temperature distributions on the middle surface of the blade.

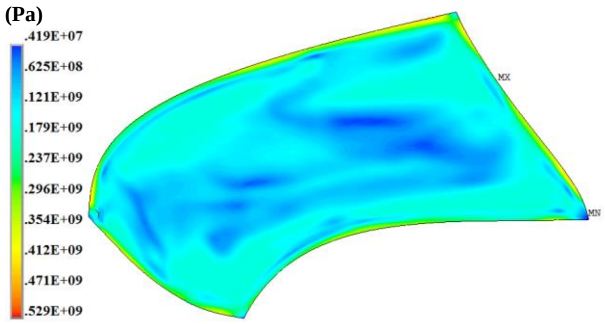


FIG. 7 –Residual von Mises stress distributions 372 seconds after cooling started.

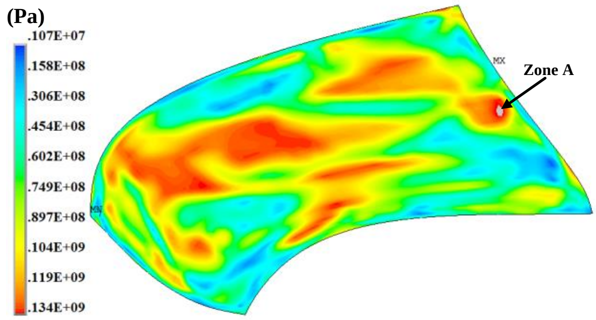


(a) Stress scale corresponding to Fig. 5

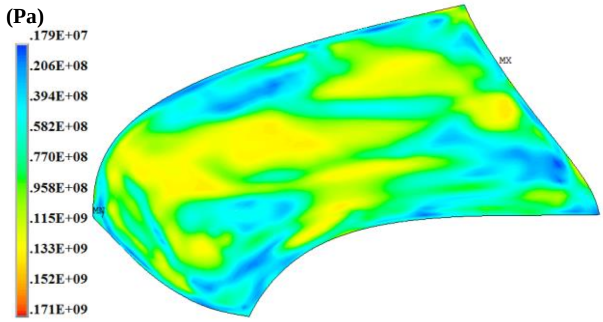


(b) Stress scale from minimal value to maximal value

FIG. 8 –Residual von Mises stress distributions after cooling finished

## 3 Conclusions

For investigating the process of manufacturing Francis turbine blades from thick plates, a numerical model using finite element approach has been built. The modelling is based on the models of the plate pressing, the springback of the pressed workpiece and the cooling of the pressed workpiece. The initial stress has been included in the history of each stage. The stress distributions have been obtained at each stage. The maximal residual stress in the final product is far below the yield stress and occurs at the maximal curvature of the workpiece. In future works, the cooling of the pressed workpiece during the forming process will be taken in account.

## References

[1] Casacci S., Caillot G., Le développement des turbomachines hydrauliques de grandes puissances, La houille blanche, 7-8, 475-484, 1983.
[2] Casacci S., Bosc J., Moulin C., Sauron, A., Conception et construction des turbomachines hydrauliques de grandes dimensions, La houille blanche 7-8, 591-616, 1977.
[3] Wang H., Djambazov G., Pericleous K.A., Harding R.A., Wickins M., Modelling the dynamics of the tilt-casting process and the effect of the mould design on the casting quality, Computers & Fluids, 42(1), 92-

101, 2011.
[4] Jayet-Gendrot, S., Gilles, P. and Migné, C., Behavior of duplex stainless steel casting defects under mechanical loadings, Nuclear Engineering and Design, 197(1–2), 141-153, 2000.
[5] Heo S.C., Kim J.N., Song W.J., Ku T.W., Kang B.S., Shape error compensation in flexible forming process using overbending surface method, International Journal of Advanced Manufacturing Technology, 59(9-12), 915-928, 2012.
[6] Heo S.C., Seo Y.H., Ku T.W., Kang B.S., A study on thick plate forming using flexible forming process and its application to a simply curved plate, International Journal of Advanced Manufacturing Technology, 51(1-4), 103-115, 2010.
[7] Walczyk D.F., Hardt D.E., Design and analysis of reconfigurable discrete dies for sheet metal forming, Journal of Manufacturing Systems, 17(6), 436-454, 1998.
[8] Feng Z., Champliaud H., Sabourin M., Morin S., Modeling and simulation based on inverse finite element method for unfolding large and thick blades of Francis turbines, Proceeding of the 24th European Modeling and Simulation Symposium, EMSS 2012, 27-31, 2012.
[9] Feng Z., Champliaud H., Mathieu L., Sabourin M., Modeling and simulation of optimal blank design and hot pressing process for manufacturing large Francis turbines blades from very thick plates, submitted to the 2013 ASME Pressure Vessels and Piping Conference, July 14-18, 2013, Paris, France.
[10] Sabourin M., Paquet F., Hazel B., Cote J., Mongenot P., Robotic approach to improve turbine surface finish,"1st International Conference on Applied Robotics for the Power Industry (CARPI 2010), October 5-7, 2010, Montreal, Canada.
[11] Deng D. and Kiyoshima S., Numerical simulation of residual stresses induced by laser beam welding in a SUS316 stainless steel pipe with considering initial residual stress influences. Nuclear Engineering and Design, 240(4), 688-696, 2010.
[12] De Strycker M., Van Paepegem W., Schueremans L., Debruyne, D., The effect of residual stresses on the strain evolution during welding of thin-walled tubes. 14th International Conference on Sheet Metal, SheMet 2011, April 18 - April 20, 2011. Leuven, Belgium: Trans Tech Publications Ltd.
[13] Park J.U., Lee H.W., Effects of initial condition of steel plate on welding deformation and residual stress due to welding. Journal of Mechanical Science and Technology, 21(3), 426-435, 2007.
[14] Huang Y., Lu H., Influence of initial stress of thin pressing parts on welding hot cracking susceptivity. Hanjie Xuebao/Transactions of the China Welding Institution, 30(2), 99-102, 2009.
[15] Sisan A.M., Motarjemi A.. The effect of strength mis-match and residual stress in ECA of girth welds with internal circumferential cracks. 2009 ASME Pressure Vessels and Piping Conference, July 26, 2009 - July 30, 2009. Prague, Czech republic: American Society of Mechanical Engineers, 2010.